Capillary Condensation of Nitrogen in MCM-48 and SBA-16

Kunimitsu Morishige,* Noriko Tateishi, and Shingo Fukuma

Department of Chemistry, Okayama University of Science, 1-1 Ridai-cho, Okayama 700-0005, Japan

Received: September 25, 2002; In Final Form: January 20, 2003

To examine the effects of connectivity among pores of almost the same size and of different size and geometry on adsorption hysteresis and pore criticality, we measured the temperature dependence of the adsorption−desorption isotherm of nitrogen onto MCM-48 and SBA-16 materials, respectively, with well-defined three-dimensional networks of cylindrical pores and cagelike pores, over a wide temperature range of $T/T_c = 0.43$ to 0.90. The results for MCM-48 strongly suggest that interconnections among pores of almost the same size and geometry do not have a significant effect on the adsorption hysteresis and pore criticality. For SBA-16 with well-defined ink-bottle pores, capillary condensation in the hysteretic isotherms takes place near the equilibrium, whereas capillary evaporation from large cavities is delayed. The classical concept of pore blocking is not supported by the experimental isotherms for SBA-16, because the delayed desorption is not concerned with emptying of the small channels. The hysteresis shrinks with increasing temperature and eventually disappears well below the bulk critical temperature, in disagreement with the classical concept of pore blocking.

I. Introduction

Capillary condensation within mesoporous materials is often distinguished by a distinct step in the adsorption isotherm accompanied by a hysteresis loop.[1] The adsorption steps are now widely used in estimating the pore size distribution of the mesoporous materials under several assumptions concerning the pore structure and the nature of adsorption and desorption branches. For unconnected cylindrical pores, it has became clear that the hysteresis results from the metastability of a confined phase and the critical temperature of vapor−liquid equilibrium (pore critical temperature, T_{cp}) is different from the temperature at which the adsorption hysteresis disappears (hysteresis critical temperature, T_{ch}).[2−5] The shifts of T_{cp} or T_{ch} relative to a bulk critical temperature (T_c) are inversely correlated to the radius of the cylindrical pores, except for large pores.[6] Capillary condensation is accompanied by the hysteresis below T_{ch}, while it occurs reversibly between T_{ch} and T_{cp}. Above T_{cp}, adsorption takes place continuously without a first-order capillary condensation.

The conventional mesoporous materials such as controlled pore glasses and silica gels have an interconnected network of pores of varying shape, curvature, and size.[7] In such systems, networking and interconnections among pores may play an important role in the adsorption hysteresis and capillary criticality. MCM-48[8] has a well-defined three-dimensional (3D) network structure of cylindrical pores as compared to the one-dimensional (1D) porous structure of MCM-41 and SBA-15. On the other hand, SBA-16 has a cagelike structure with a cubic symmetry. A high-resolution electron microscopic study[9] has revealed that spherical cavities of 9.5 nm diameter are arranged in a body-centered cubic array and the cavities are connected through small channels of 2.3 nm along the [111] direction. Therefore, MCM-48 and SBA-16 present good candidates for examining the effects of connectivity among pores of almost the same size and of different size and geometry, respectively, on the adsorption hysteresis and pore criticality. To elucidate these effects, we measured the temperature dependence of the adsorption−desorption isotherm of nitrogen onto MCM-48 and SBA-16 over a wide temperature range of $T/T_c = 0.43$ to 0.90.

II. Experiment

The synthesis of siliceous MCM-48 is based on the procedure of Beck et al.[10] Sodium silicate, water, and trimethylstearylammonium chloride were combined with stirring. After the resulting mixture was allowed to stir for several minutes, pyrogenic silica and tetramethylammonium hydroxide solution were added, and the resulting gel was allowed to stir for another several minutes. The gel was heated in a sealed Pyrex-glass tube at 393 K for 24 h. The washed and then dried products were calcined at 813 K for 8 h in flowing air. The calcined material gave a well-defined XRD pattern typical of a MCM-48 mesoporous molecular sieve. The pore size was determined from comparing the relative pressure of equilibrium transition of nitrogen at 77 K with that calculated on the basis of nonlocal density functional theory (NLDFT)[11] for the cylindrical pores of siliceous mesoporous materials: $r_p = 1.9$ nm. SBA-16 was prepared using Pluronic F127 triblock copolymer according to the procedure of Zhao et al.[12] The template was removed from SBA-16 by heating at 413 K for 3 h and then at 823 K for 4 h in flowing air. The XRD pattern of the calcined material showed a broad (200) reflection of a cubic SBA-16. This indicates that the quality of our sample is inferior to that of Zhao et al.,[12] although the shape of the adsorption isotherm of nitrogen at 77 K for our sample was almost the same as that of their sample.

Adsorption isotherms were measured volumetrically on a homemade semi-automated instrument equipped with a Baratron capacitance manometer (Model 690A) with a full scale of 25000 Torr,[6] except for low temperatures. A few isotherms at low temperatures were measured on the same type of instrument equipped with a capacitance manometer with a full scale of 100 Torr. The temperature of the substrate was estimated from the saturated vapor pressure of nitrogen inside the sample cell.[6,13]

* Corresponding author. Tel: 086-256-9494. Fax: 086-256-2891. E-mail: morishi@chem.ous.ac.jp.

10.1021/jp022137c CCC: $25.00
Published on Web 05/09/2003

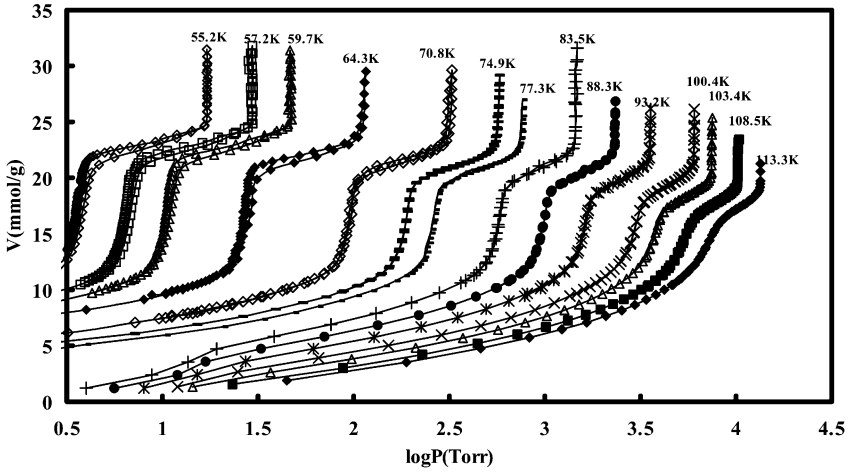

Figure 1. Temperature dependence of the adsorption−desorption isotherm of nitrogen onto MCM-48.

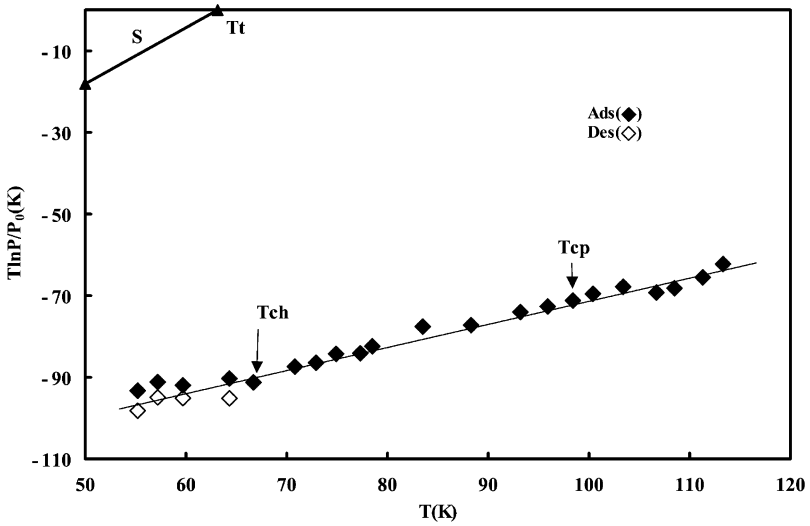

Figure 2. Temperature dependence of the capillary condensation and evaporation pressures of nitrogen onto MCM-48.

Calculation of adsorption at higher pressures took nonideality of gas into consideration on the basis of a modified BWR equation.[13]

Results and Discussion

A. MCM-48. The MCM-48 ordered mesoporous silica has the cubic space-group symmetry of *Ia*3*d*, and the wall surface follows exactly the periodic minimal surface of gyroid.[8] The wall separates two interpenetrating and noninterconnecting channel systems with different chiralities. Each forms a three-dimensional (3D) network with channels running along [111] and [100] and thus the MCM-48 gives a model adsorbent most suitable to elucidate the effects of networking and interconnections among pores of almost the same size and geometry on capillary condensation and pore criticality. It can be regarded as the special case of the cagelike structure having the same size of cavities as that of windows. Gelb et al.[7] have suggested that interconnections among pores may have a significant effect on the location of the pore critical point (T_{cp}), because near pore connection points the correlation length can grow to lengths greater than the pore width in the direction different from the pore axis, as the T_{cp} is approached by raising the temperature.

Figure 1 shows the temperature dependence of the adsorption−desorption isotherm of nitrogen onto MCM-48 in the temperature range 55−113 K. When the temperature was raised, the hysteresis loop shrank and eventually disappeared, as usually observed for mesoporous materials. T_{ch} can be taken as the temperature at which the hysteresis loop vanishes: $T_{ch} \sim 67$ K. The shape of the hysteresis loop and the thermal behavior of the isotherm were similar to those found for MCM-41[6] with unconnected cylindrical pores. Figure 2 shows the plots of the capillary condensation and evaporation pressures against temperature. Here, the condensation and evaporation pressures were determined at the midpoint of the adsorption and desorption steps, respectively, and P_0 is the saturated vapor pressure of the bulk liquid. At lower temperatures $T \ln(P/P_0)$ is the difference of the chemical potential with respect to the bulk liquid. This figure includes the data of T_{ch} and T_{cp}. The determination of T_{cp} will be described in a subsequent section. As Figure 2 shows, a plot of $T \ln(P/P_0)$ vs T for capillary condensation forms an almost linear relationship over a wide temperature range. This is in sharp contrast with the relationship observed on MCM-41, where the temperature dependence of the equilibrium condensation pressure suddenly changed around 94 K.[6]

T_{cp} was determined from the inflection point in a plot of $(\partial(P/P_0)/\partial V)_T$ estimated at the midpoint of the adsorption step against temperature.[3] It is expected that above T_{cp} $(\partial(P/P_0)/\partial V)_T$ increases rapidly while at lower temperatures it keeps a low value, although its true behavior is somewhat obscure. In true first-order transition of capillary condensation, $(\partial(P/P_0)/\partial V)_T$ vanishes. In real porous materials, however, nonuniformity of

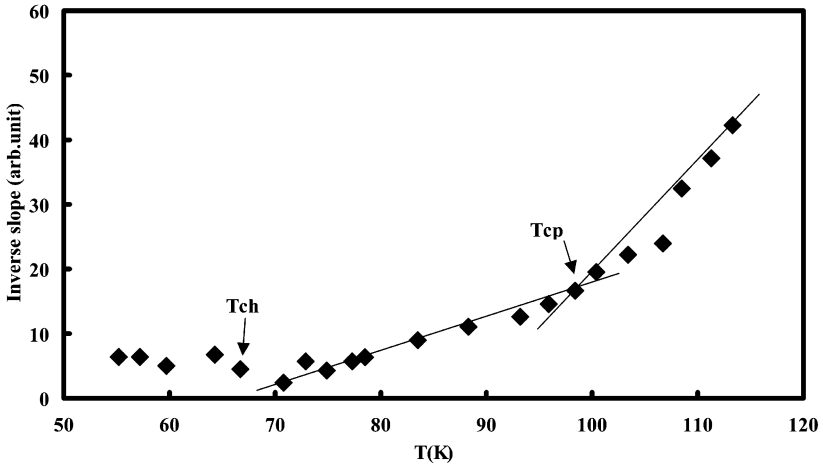

Figure 3. Temperature dependence of the inverse slope of the adsorption step associated with capillary condensation of nitrogen onto MCM-48. Solid lines are guides for the eye.

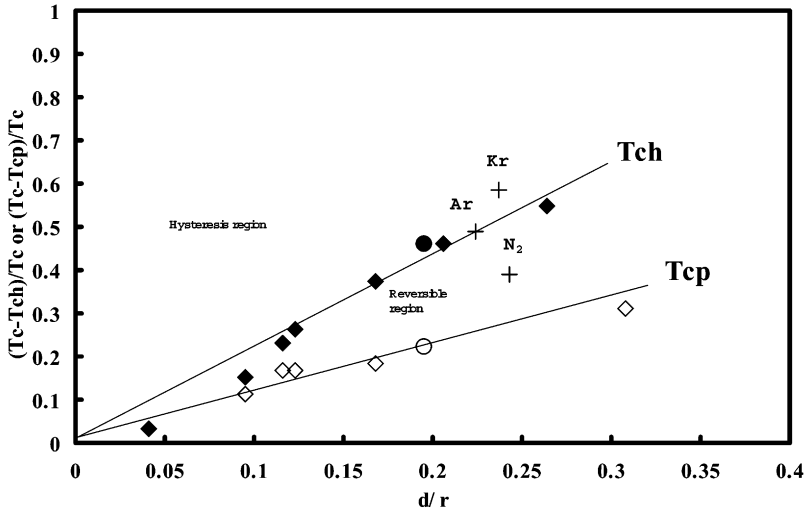

Figure 4. Plots of $(T_c - T_{ch})/T_c$ and $(T_c - T_{cp})/T_c$ against d/r_p for nitrogen in independent and interconnected cylindrical pores. MCM-41 and SBA-15(◇,◆) and MCM-48(○,●). Crosses denote the experimental conditions of Thommes et al.[14] for MCM-48. Solid lines are guides for the eye.

pore size distribution smears out the first-order transition and results in nonverticality of the step associated with capillary condensation. Although such a procedure is empirical, recent simulations[5] have shown that the value of T_{cp} of Ar on MCM-41 of $r_p = 1.2$ nm determined in such a way is in good agreement with that estimated from the gauge cell method. As Figure 3 shows, a plot of $(\partial(P/P_0)/\partial V)_T$ vs T did not break upward at T_{ch}. If T_{ch} was equal to T_{cp}, this plot would break at T_{ch}. Evidently, in the pores of MCM-48, T_{ch} is not equal to T_{cp}. This plot broke around 98 K. Therefore, we consider that this temperature is T_{cp} for the present system. T_{ch} and T_{cp} of nitrogen for the interconnected pores of MCM-48 are compared to those for the unconnected cylindrical pores[6] of MCM-41 and SBA-15 in Figure 4. This figure shows the plots of $(T_c - T_{ch})/T_c$ and $(T_c - T_{cp})/T_c$ against d/r_p, where d is taken from the size parameter (0.37 nm) of nitrogen for the Lennard-Jones potential. The data points for MCM-48 did not deviate from the almost linear relationship between the critical point shifts and the reciprocal pore-radius observed for MCM-41 and SBA-15. This strongly suggests that interconnections among pores of almost the same size and geometry do not have a significant effect on the adsorption hysteresis and capillary criticality. This is in accord with the implication by Schumacher et al.[11] Thommes et al.[14] have reported that the isotherms of Ar at 77 K and of Kr at 87 K on MCM-48 reveal the hysteresis loop, whereas that of N_2 at 77 K is reversible. These observations can be well understood in the framework of the relationship between T_{ch} and pore size shown in Figure 4. This figure includes the experimental conditions for N_2 and Ar at 77 K and for Kr at 87 K on sample C of their MCM-48 materials in a temperature−d/r plot. The data points for Ar and Kr are located within the hysteresis region whereas that of N_2 is located within the reversible isotherm region.

B. SBA-16. The SBA-16 ordered mesoporous silica has the cubic space-group symmetry of *Im*3*m*, and the wall surface follows the periodic minimal surface of I-WP (body centered, wrapped package).[9,15] This cagelike structure exactly corresponds to the so-called "ink-bottle" pore model. The concept of hysteresis in this kind of a pore is based on the assumption that desorption from a cavity is delayed until the vapor pressure is reduced below the equilibrium desorption pressure from the pore window (pore blocking effects).[16] Very recently, however, molecular dynamics simulations[17] and nonlocal density functional theory (NLDFT)[15] have shown that the classical picture of adsorption and desorption in this geometry based on the concept of pore blocking does not necessarily hold.

Figure 5 shows the temperature dependence of the adsorption−desorption isotherm of nitrogen onto SBA-16 in the temperature range 53−113 K. At lower temperatures, the isotherms exhibited large hysteresis loops of type H2 in the

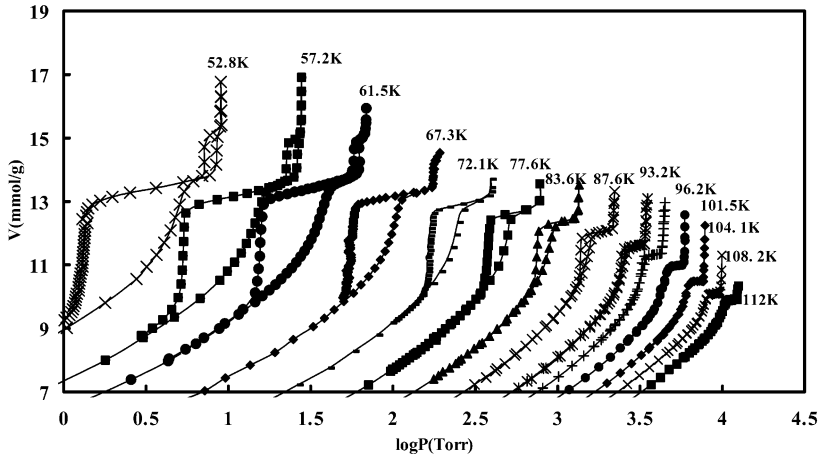

Figure 5. Temperature dependence of the adsorption−desorption isotherm of nitrogen onto SBA-16.

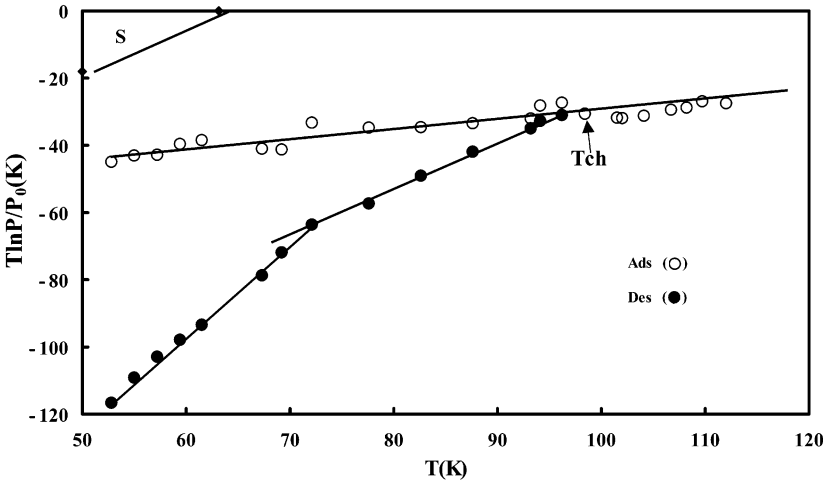

Figure 6. Temperature dependence of the capillary condensation and evaporation pressures of nitrogen onto SBA-16.

IUPAC classification,[18] similar to those for disordered mesoporous materials such as porous glasses and silica gels. This type of hysteresis is characterized by a steep desorption branch and a smoothly increasing adsorption branch. The smoothly increasing adsorption branch has been traditionally ascribed to a pore size distribution of conventional mesoporous materials. The steep desorption branch has often been ascribed to pore blocking effects of the liquid confined within windows connecting larger cavities. The equilibrium evaporation pressure (relative pressure p/p_0) of liquid nitrogen confined within the windows of 2.3 nm at 77 K is estimated to be ~0.15 from pore-size dependence of the N_2 adsorption step on MCM-41 with cylindrical pores.[19,20] This value is substantially lower than the position ($p/p_0 = 0.47$) of the desorption branch observed here. Therefore, the classical concept of pore blocking is not supported by the experimental isotherms for SBA-16 having well-defined ink-bottle pores. Instead, it is indicated that the fluid in the large cavities of SBA-16 becomes thermodynamically unstable at a higher pressure than the equilibrium desorption pressure for the pore windows and thus the confined fluid desorbs via spontaneous cavitation. When the temperature was increased, the hysteresis loop shrank and eventually disappeared at 98 K. The disappearance of the hysteresis loop with increasing temperature cannot be accounted for by the classical concept of pore blockings. Thermal behavior of the hysteresis loop was also similar to that observed for the conventional mesoporous materials. This suggests that the pore structure of the conventional mesoporous materials such as porous glasses can be regarded as a network of cavities interconnected through smaller necks. At lower temperatures, a small hysteresis loop appeared near the saturated vapor pressure. As the substrate used in the measurements at lower temperatures was a self-supporting disk made from compression of the powder, interparticle voids might be responsible for it.

Figure 6 shows the plots of the capillary condensation and evaporation pressures against temperature for nitrogen on SBA-16. Here the evaporation pressure was determined at the midpoint of the desorption branch while the condensation pressure was estimated at the steepest point of the adsorption branch. The plot for capillary condensation formed an almost linear relationship over a wide temperature range including T_{ch}. This indicates that capillary condensation in the hysteretic isotherms takes place near the equilibrium. Very recently, Ravikowitch and Neimark[15] have reported the pore size dependence for the equilibrium capillary condensation pressure of nitrogen at 77 K in spherical pores of siliceous materials due to NLDFT. Therefore, we are able to estimate the cavity size of our SBA-16 sample from comparing the experimental adsorption branch at 77 K with the relationship between the equilibrium transition pressure and the diameter of spherical pores reported by them. It gives the cavity size to be 9.2 nm. This is in excellent agreement with the estimate (9.5 nm) obtained from the high-resolution electron microscopic study.[9] On the other hand, the evaporation pressures of the confined nitrogen in the hysteretic isotherms deviated significantly from the temperature dependence of the equilibrium evaporation

pressure measured above T_{ch}. This clearly indicates that desorption from large cavities is delayed. This delayed desorption is not concerned with emptying of the small channels. The extent of metastability of the liquid confined to large cavities decreases with increasing temperature and disappears at 98 K. In addition, the temperature dependence of the irreversible capillary evaporation pressure suddenly changed around 72 K. This change is not concerned with the phase change of liquid nitrogen within large cavities, although a similar change in the temperature dependence of capillary condensation and evaporation pressures has been often observed on freezing of a confined phase.[21] T_{cp} for the present system was not estimated, because the adsorption branch was not steep.

On adsorption, layering of molecules on the wall of both the large cavities and the small channels first takes place. This continues until the small channels are filled with fluid. Further increase of the vapor pressure results in diffusion of fluid into the large cavities and finally vapor bubbles remain inside the large cavities. The steepest part of the adsorption branch is associated with the disappearance of the vapor bubbles, namely the capillary condensation of nitrogen. On desorption, the large cavities remain filled with liquid until lower pressures relative to those where the capillary condensation occurred. Then evaporation of fluid from the large cavities takes place while the small channels remain filled with fluid. Hysteresis occurs because on desorption there is essentially nothing in the system to nucleate a large-scale evaporation process in the large cavity until the pore liquid reaches a sufficiently expanded state that spontaneous local density fluctuations can lead to cavitation.[15,17] The formation and disappearance of the vapor bubble resembles the freezing and melting of a nanoparticle. The formation of the vapor bubble requires a kinetic energy for homogeneous nucleation and thus the liquid confined to the large cavities is easy to become metastable. On the other hand, the disappearance of the vapor bubble would take place near the thermodynamic equilibrium, similar to the melting of the nanoparticle, because it does not need a nucleation process. Therefore, the capillary condensation takes place near the equilibrium, whereas the capillary evaporation takes place near the liquidlike spinodal.

Acknowledgment. This work was supported by the Grant-in-Aid for Scientific Research, No.12440201, provided by the Ministry of Education, Culture, Sports, Science and Technology of Japan and by Okayama Foundation for Science and Technology. The authors thank BASF-Japan (Tokyo) for donating the block copolymer surfactant Pluronic used in this study.

References and Notes

(1) Gregg, S. J.; Sing, K. S. W. *Adsorption, Surface Area, and Porosity*; Academic: New York, 1982.

(2) Ravikowitch, P. I.; Domhnail, S. C. O.; Neimark, A. V.; Schuth, F.; Unger, K. K. *Langmuir* **1995**, *11*, 4765.

(3) Morishige, K.; Shikimi, M. *J. Chem. Phys.* **1988**, *108*, 7821.

(4) Sonwane, C. G.; Bhatia, S. K. *Langmuir* **1999**, *15*, 5347.

(5) Vishnyakov, A.; Neimark, A. V. *J. Phys. Chem. B* **2001**, *105*, 7009.

(6) Morishige, K.; Ito, M. J. *Chem. Phys.* **2002**, *117*, 8036.

(7) Gelb, L. D.; Gubbins, K. E.; Radhakrishnan, R.; Sliwinska-Bartkowiak, M. *Rep. Prog. Phys.* **1999**, *62*, 1573.

(8) Kaneda, M.; Tsubakiyama, T.; Carlsson, A.; Sakamoto, Y.; Ohsuna, T.; Terasaki, O.; Joo, S. H.; Ryoo, R. *J. Phys. Chem. B* **2002**, *106*, 1256.

(9) Sakamoto, Y.; Kaneda, M.; Terasaki, O.; Zhao, D. Y.; Kim, J. M.; Stucky, G.; Shin, H. J.; Ryoo, R. *Nature* **2000**, *408*, 449.

(10) Beck, J. S.; Vartuli, J. C.; Roth, W. J.; Leonowicz, M. E.; Kresge, C. T.; Schmitt, K. D.; Chu, C. T.-W.; Olson, D. H.; Sheppard, E/W.; McCullen, S. B.; Higgins, J. B.; Schlenker, J. L. *J. Am. Chem. Soc.* **1992**, *114*, 10834.

(11) Schumacher, K.; Ravikowitch, P. I.; Chesne, A. D.; Neimark, A. V.; Unger, K. K. *Langmuir* **2000**, *16*, 4648.

(12) Zhao, D.; Huo, Q.; Feng, J.; Chmelka, B. F.; Stucky, G. D. *J. Am. Chem. Soc.* **1998**, *120*, 6024.

(13) Younglove, B. A. *J. Phys. Chem. Ref. Data* **1982**, *11*, Suppl.1.

(14) Thommes, M.; Kohn, R.; Froba, M. *J. Phys. Chem. B* **2000**, *104*, 7932.

(15) Ravikowitch, P.; Neimark, A. V. *Langmuir* **2002**, *18*, 1550.

(16) Mason, G. *Proc. R. Soc. London, Ser. A* **1988**, *415*, 453.

(17) Sarkisov, L.; Monson, P. A. *Langmuir* **2001**, *17*, 7600.

(18) Sing, K. S. W.; Everett, D. H.; Haul, R. A.; Moscou, L.; Pierotti, R. A.; Rouquerol, J.; Siemieniewska, T. *Pure Appl. Chem.* **1985**, *57*, 603.

(19) Neimark, A. V.; Ravikowitch, P. I. *Microporous Mesoporous Mater.* **2001**, *44*, 697.

(20) Morishige, K.; Fujii, H.; Uga, M.; Kinukawa, D. *Langmuir* **1997**, *13*, 3494.

(21) Huber, P.; Knorr, K. *Phys. Rev. B* **1999**, *60*, 12657.